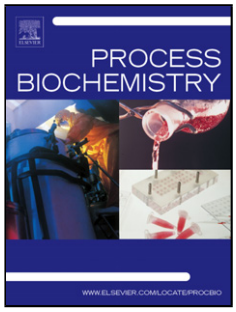

Title: Coupled (*R*)-carbonyl reductase and glucose dehydrogenase catalyzes (*R*)-1-phenyl-1,2-ethanediol biosynthesis with excellent stereochemical selectivity

Author: Xiaotian Zhou Rongzhen Zhang Yan Xu Hongbo Liang Jiawei Jiang Rong Xiao

PII: S1359-5113(15)30056-8
DOI: http://dx.doi.org/doi:10.1016/j.procbio.2015.08.002
Reference: PRBI 10491

To appear in: *Process Biochemistry*

Received date: 15-4-2015
Revised date: 10-6-2015
Accepted date: 2-8-2015

Please cite this article as: Zhou Xiaotian, Zhang Rongzhen, Xu Yan, Liang Hongbo, Jiang Jiawei, Xiao Rong.Coupled (R)-carbonyl reductase and glucose dehydrogenase catalyzes (R)-1-phenyl-1,2-ethanediol biosynthesis with excellent stereochemical selectivity.*Process Biochemistry* http://dx.doi.org/10.1016/j.procbio.2015.08.002

Coupled (*R*)-carbonyl reductase and glucose dehydrogenase catalyzes (*R*)-1-phenyl-1,2-ethanediol biosynthesis with excellent stereochemical selectivity

Xiaotian Zhou [a], Rongzhen Zhang [a,b*], Yan Xu [a,b*], Hongbo Liang [a], Jiawei Jiang[a], Rong Xiao [c]

[a] Key Laboratory of Industrial Biotechnology of Ministry of Education & School of Biotechnology, Jiangnan University, Wuxi 214122, P. R. China

[b] National Key Laboratory for Food Science, Jiangnan University, Wuxi 214122, P. R. China

[c] Center for Advanced Biotechnology and Medicine, Rutgers University, Piscataway, NJ 08854, USA

***Corresponding authors: Rongzhen Zhang and Yan Xu**

Tel: +86-510-85197760; Fax: +86-510-85864112

Address correspondence to: Rongzhen Zhang, rzzhang@jiangnan.edu.cn; and Yan Xu, yxu@jiangnan.edu.cn

Present address: School of Biotechnology, Jiangnan University, 1800 Lihu Avenue, Wuxi 214122, P. R. China

Graphical abstract

The coupled system based on RCR and GDH was rebalanced through protein-expression optimization. It gave excellent performance on (*R*)-PED biotransformation without exogenous cofactors.

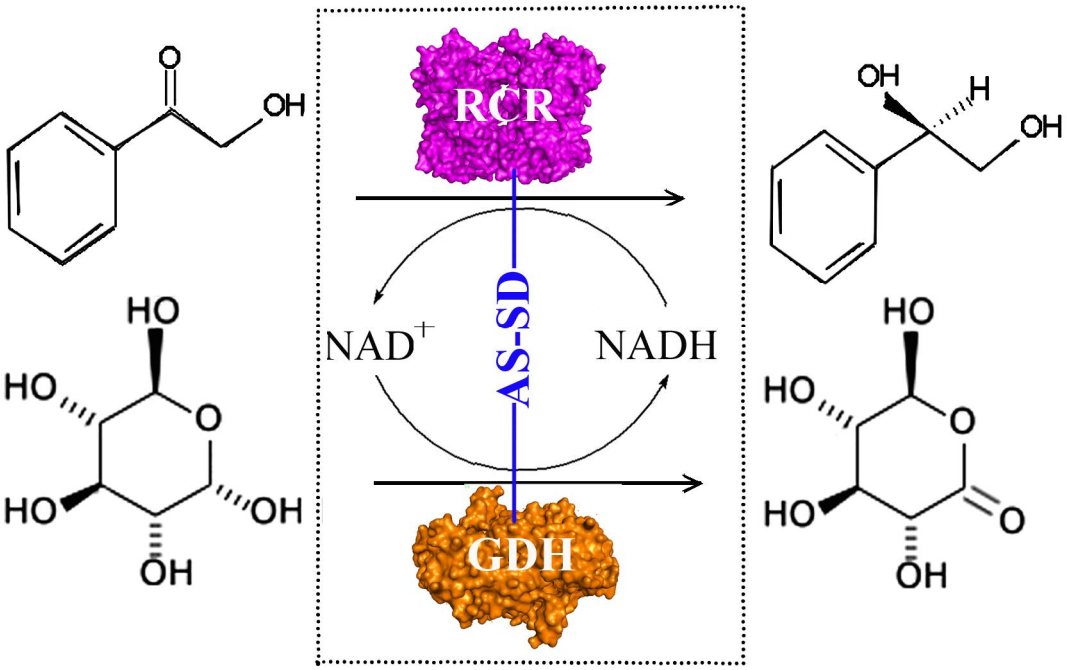

Highlights:

1. The construction of coupling system contain RCR and GDH
2. The introduction of GDH has little effects on cell-growth
3. The functions of RCR and GDH were rebalanced through protein-expression optimization
4. The coupling system produced (*R*)-PED with excellent stereochemical selectivity

Abstract:

The biotransformation of 2-hydroxyacetophenone to (*R*)-1-phenyl-1, 2-ethanediol (PED) by NADH-dependent (*R*)-carbonyl reductase (RCR) from *Candida parapsilosis* is slow and gives low yields, probably as a result of insufficient cofactors. To improve the biotransformation efficiency of (*R*)-PED from 2-hydroxyacetophenon, an enzyme-coupling system containing RCR and glucose dehydrogenase (GDH) was constructed to strengthen NADH-recycling pathway in *Escherichia coli*, in which the Shine–Dalgarno sequence and the aligned spacing sequence were used as linkers between them. The introduction of glucose dehydrogenase had little affects on the cell-growth. The co-expression conditions of RCR and glucose dehydrogenase was optimized to rebalance their catalytic functions. The ratio of k_{cat}/K_M for enzyme-coupling system catalyzing 2-HAP and glucose was about 1.0, suggesting the good balance between the functions of RCR and GDH. The rebalanced system gave excellent performance in (*R*)-PED biotransformation: an optical purity of 99.9% and a yield of 99.9% at optimal conditions: 35 °C and pH 7.0. The introduction of glucose dehydrogenase stimulated increases of 23.8% and 63.8%, in optical purity and yield of (*R*)-PED, and simultaneously reduced the reaction time two-fold. This work provided a valuable method for efficient chiral alcohol production through protein-expression and biotransformation optimization to rebalance cofactor pathways.

Keywords: (*R*)-1-phenyl-1, 2-ethanediol, (*R*)-carbonyl reductase, NADH regeneration, glucose dehydrogenase, *Candida parapsilosis*

Abbreviations: GDH, Glucose dehydrogenase; 2-HAP, 2-hydroxyacetophenone;

RCR, (*R*)-carbonyl reductase; (*R*)-PED, (*R*)-1-phenyl-1, 2-ethanediol; (*S*)-PED, (*S*)-1-phenyl-1, 2-ethanediol

1. Introduction

Optically active alcohols are very useful chiral blocks in the special chemical and pharmaceutical industries [1, 2]. For example, (*R*)-1-phenyl-1, 2-ethanediol (PED) can be used for synthesis of an antidepressant drug, fluoxetine, which extends the effects of 5-hydroxy tryptamine through selective inhibition for the extraction of 5-hydroxy tryptamine in central nervous system [3]. With the increasing requirement of chiral compounds in different fields, people pay more and more attentions to high optical purity and yield of enantiopure chemicals [4-6]. The efficient preparation of single enantiomers has become a hot research in recent years [7-9].

The cofactor-dependent asymmetric reduction of ketones catalyzed by alcohol dehydrogenases, is a valuable method for the synthesis of optically active alcohols [10-12]. It was reported that carbonyl reductase from *Aspergillus niger*, *Candida tropicalis*, *Rhizopus arrhizus*, *Ralstonia* sp., *Rhodotorula glutinis*, *Trichothecium* sp. *et al*. efficiently catalyzes prochiral substrate into the corresponding chiral products [13-18]. *Candida parapsilosis* (*S*)-carbonyl reductase gives good performance in the reduction of 2-hydroxyacetophenone (HAP) to (*S*)-PED. However, with the increase of substrate concentrations, protons transfer of cofactor NAD(P)(H) will be a restriction factor during alcohol dehydrogenase-mediated biotransformation [19]. The construction of enzyme-coupled system to introduce cofactor-regeneration enzyme is an attractive technique to improve chiral biosynthesis [20].

There are several enzymes involved in NAD(P)(H) recycling, such as formate dehydrogenase, glucose dehydrogenase (GDH), and alcohol dehydrogenases [21-23].

The enzyme GDH is one of the most frequently used cofactor-regeneration enzymes because it can regenerate both NADPH and NADH [24,25]. There are several advantages in the GDH-mediated cofactor-regeneration system as follows: GDH is characterized with favourable thermodynamics, and it has high enzyme activity over a broad pH range and high stability against several organic compounds [24-26]; The hydride source is cheap glucose; And glucose/gluconic acid produced by the system does not interfere with the synthesis reaction [23]. For example, Zhang *et al.* efficiently produced (*S*)-PED with optical purity of over 99% in a yield of 96% by introduction of *Bacillus* sp. YX-1 GDH into (*S*)-carbonyl reductase-mediated biotransformation pathway [27]. Xiao *et al.* reported a novel whole-cell biotransformation containing GDH for NAD^+ regeneration to prepare chiral chemicals [28]. Kosjek *et al.* realized efficient preparation of 4, 4-dimethoxytetrahydro-2H-pyran-3-ol and (*S*)-4-chloro-3-hydroxybutanoate using coupled systems consisting of carbonyl reductase and GDH [29-31].

In our previous work, we reported an NADH-dependent (*R*)-carbonyl reductase (RCR, also named (*R*)-alcohol dehydrogenase) from *C. parapsilosis* catalyzing the reduction of 2-hydroxyacetophenone (2-HAP) to (*R*)-PED [32, 33]. Very recently, we determined crystal structure of RCR and its catalytic mechanism of stereoselectivity [34]. However, the recombinant *Escherichia coli*-RCR catalyzed the transformation of (*R*)-PED with an optical purity of 81% in a yield of 61% [35]. The low biotransformation efficiency may be due to insufficient cofactors or weak cofactor-regeneration pathway [36]. By replacing the protein expression hosts, the

recombinant RCR still produced (*R*)-PED with unsatisfied efficiency in *Saccharomyces cerevisiae* and *Pichia pastoris* [33, 37]. Wang *et al.* significantly improved the biotransformation efficiency of (*R*)-PED through the addition of glycerol and isopropol into the reaction system by a dual-cosubstrate-coupled system, but the chiral synthesis is not clean process [11]. In this work, to realize the efficient preparation of (*R*)-PED with a higher optical purity by RCR, we introduced GDH from *Bacillus* sp. YX-1 to strengthen cofactor regeneration during RCR-catalyzed biotransformation in *E. coli*. The coupled system containing RCR and GDH gives excellent performance in producing (*R*)-PED with almost absolute stereochemical selectivity.

2. Materials and Methods

2.1 Microorganisms and chemicals

The PrimeSTAR® HS, pMD19-T vector, restriction enzymes and T4 DNA ligase were bought from Takara (Otsu, Japan). 2-HAP was purchased from TCI Development Co. Ltd. (Shanghai, China). (*R*)-PED, (*S*)-PED and NADH were purchased from Sigma-Aldrich (St. Louis, USA). Hexane and isopropanol used for high performance liquid chromatography (HPLC) were of chromatographic grade from Sigma-Aldrich (St. Louis, USA). All other chemicals used were of analytical grade and commercially available. The organisms were cultivated as described previously [12]. The strains used in this work are listed in Table 1.

Insert Table 1

2.2 Construction of co-expression system of RCR and GDH

The co-expression system containing RCR and GDH were constructed using a Shine–Dalgarno and aligned spacing sequence (GAAGGAGATATACC) as a linker between them. The fusion gene RCR-SD-AS-GDH was cloned using a modified overlap-extension technique on plasmid pET-28a(+) [38]. The recombinant plasmid pET-R-SD-AS-G was transformed into the competent *E. coli* BL21 (DE3), *E. coli* RIL and *E. coli* Rosetta cells chemically, and the positive *E. coli* BL21/pET-R-SD-AS-G, *E. coli* RIL/pET-R-SD-AS-G and *E. coli* Rosetta/pET-R-SD-AS-G clones were verified by DNA determination. The plasmids and primers used were listed in Table 1.

2.3 Protein expression

The recombinant strains *E. coli* BL21/pET-R-SD-AS-G, *E. coli* RIL/pET-R-SD-AS-G and *E. coli* Rosetta/pET-R-SD-AS-G were grown in LB medium containing 50 $\mu g ml^{-1}$ kanamycin at 37°C. When OD_{600} value of the culture reached 0.8, isopropyl-β-D-thiogalactopyranoside (IPTG) of 0.5 mM was added to induce protein expression. The cultures were cultivated at 37°C for 16 h and then harvested by centrifugation.

The protein expression of RCR and GDH was optimized under the different OD_{600} value (0.4-1.5) of the culture, different IPTG concentrations (0.2-2.0 mM), different induce temperature (17°C -37°C), different induce times (8-20 h).

2.4 Protein purification

The harvested cells were resuspended in 0.1 M potassium phosphate buffer (pH 7.0) and lysed by sonication with an ultrasonic oscillator (Sonic Materials Co., USA), The cell debris were removed by centrifugation (12000×g, 40 min) at 4°C, and the supernatant was applied to a HisTrap HP affinity column (GE Healthcare, Piscataway, NJ, USA) equilibrated with a buffer (20 mM Tris-HCl, 0.3 M NaCl; pH 7.5), and then was eluted with a buffer (20 mM Tris-HCl, 0.3 M NaCl, 0.3 M imidazole; pH 7.5) using an ÄKTA purifier system (GE Healthcare, Piscataway, USA). The homogeneity of purified enzymes was judged by Coomassie brilliant blue staining of SDS-PAGE gels.

2.5 Enzyme assay

The reduction activities of RCR were measured at 35°C and pH 7.0 by spectrophotometrically recording the rate of change of NADH absorbance at 340 nm. One unit of enzyme activity is defined as the amount of enzyme catalyzing the oxidation of 1 μmol of NADH per minute under the measurement conditions. The standard assays were performed as described by Nie *et al.* [39]. The oxidation activities of GDH were measured at 35°C and pH7.0 by spectrophotometrically recording the rate of change of NADH absorbance at 340 nm. One unit of enzyme activity is defined as the amount of enzyme catalyzing the reduction of 1 μmol of NAD^+ per minute under the measurement conditions. The protein concentration was determined by the Bradford method with bovine serum albumin as the standard.

2.6 Kinetic parameters

Various concentrations of substrate 2-hydroxyacetophenone (0.05–0.5 mM), enzyme (10–200 μM), and cofactors NADH (0.05–0.5 mM) in 100 mM phosphate buffer (pH 7.5) were used for kinetic parameters determination [40]. The data were fitted to the Michaelis–Menten equation by using a nonlinear least-square iterative method using KaleidaGraph (Synergy Software, Reading, PA). Three sets of kinetic parameters were obtained from three independent experiments and then simply averaged to yield the final estimates. The final estimates are shown with the standard errors for the three sets.

2.7 Biotransformation and analytical methods

The bioconversion mixture (2 mL) consisted of 0.1 M potassium phosphate buffer (pH 7.0), 6 gL^{-1} 2-HAP, 12 gL^{-1} glucose, and 0.1 g washed wet cells. The reactions were carried out at 35°C for 36 h with shaking at 200 rpm. After the cells were removed by centrifugation, the supernatant was extracted with ethyl acetate., and the organic layer was filtered through a 0.22 μm PVDF syringe filter (Troody Technology, Shanghai, China) for analysis. The optical purity and yield of (*R*)-PED were determined by HPLC (HP 1100, Agilent, USA) equipped with a Chiralcel OB-H column (4.6 mm ×250 mm; Daicel Chemical Ind., Ltd., Japan) as described by Nie *et al.* [39].

2.8 Optimal pH and temperature

The pH optimum of (*R*)-PED transformation was determined between pH 4.0 and 10.0 using 0.1 M citric acid buffer (pH 4.0, 4.5, 5.0, 5.5), 0.1 M potassium phosphate buffer (pH 6.0, 6.5, 7.0, 7.5), 50 mM Tris-HCl buffer (8.0), and 0.1 M carbonate buffer (pH 9.0, 10.0).

The temperature optimum of (*R*)-PED transformation was determined at various temperatures (20°C–80°C). The biotransformation of (*R*)-PED was determined with the standard assay method described above.

3. Results and discussion

3.1 Construction of the coupled-system containing RCR and GDH

The recombinant *E. coli*-RCR catalyzes the reduction of 2-HAP to (*R*)-PED with low optical purity and yield, probably as a result of insufficient cofactors or weak cofactor-recycling pathway [12]. To improve the biotransformation efficiency of (*R*)-PED, the introduction of cofactor-regeneration enzyme GDH into the reaction system would be a good strategy [24]. In this work, the RCR and GDH genes were cloned with the Shine–Dalgarno sequence and the aligned spacing sequence (GAAGGAGATATACC) as a linker between them. The fusion gene RCR-AS-SD-GDH was cloned on pET-28a plasmid to construct the recombinant plasmid pET-R-SD-AS-G. Since there are a few rare codons in RCR gene, *E. coli* BL21, *E. coli* Rosetta and *E. coli* RIL were used as hosts for co-expression of RCR and GDH. The recombinant plasmid pET-R-SD-AS-G was transformed into three kinds of

hosts: *E. coli* BL21, *E. coli* RIL and *E. coli* Rosetta, and the corresponding strains *E. coli* BL21/pET-R-SD-AS-G, *E. coli* RIL/pET-R-SD-AS-G and *E. coli* Rosetta/pET-R-SD-AS-G were obtained and then confirmed by DNA sequencing.

3.2 Co-expression of RCR and GDH

The three recombinant cells *E. coli* BL21/pET-R-SD-AS-G, *E. coli* RIL/pET-R-SD-AS-G and *E. coli* Rosetta/pET-R-SD-AS-G were induced with 0.5 mM isopropyl-β-thiogalactopyranoside (IPTG) and supplied for SDS-PAGE analysis. SDS-PAGE analysis results showed that two apparent bands corresponding to the expected sizes (44 kDa and 30 kDa) of the target recombinant enzymes, RCR and GDH, were observed in all recombinant cell extracts (Fig. 1). The cell-free extracts of recombinant *E. coli* BL21/pET-R-SD-AS-G, *E. coli* RIL/pET-R-SD-AS-G and *E. coli* Rosetta/pET-R-SD-AS-G showed reductive activities of 0.6 Umg^{-1}, 0.6 Umg^{-1} and 0.4 Umg^{-1} with 2-HAP as substrate, and 1.1 Umg^{-1}, 1.3 Umg^{-1} and 0.9 Umg^{-1} with glucose as substrate, respectively (Table 2). The three recombinant strains catalyzes the reduction of 2-HAP to (*R*)-PED with optical purity of 45.1%, 96.1% and 87.9%, in yields of 20.4%, 63.8% and 60.2%, at 35°C and pH 7.0. From these above results, *E. coli* RIL/pET-R-SD-AS-G shows the highest specific activity and biotransformation efficiency of (*R*)-PED among the three recombinant strains.

Insert Fig. 1

Insert Table 2

3.3 Introduction of GDH had little effect on cell growth

The cofactor regeneration enzyme, GDH, involved in glucose metabolic pathway, catalyzes glucose to glucono-δ-lactone, which maybe affect the grow properties of recombinant cells. We determined the cell-growth properties by measuring the turbidity of the culture at OD_{600} using a UV–visible spectroscopy system (Fig. 2). Based on the curves, the recombinant strain *E. coli* RIL/pET-R-SD-AS-G grew at a similar rate compared with *E. coli* RIL/pET-RCR, *E. coli* RIL/pET-GDH and the control strain *E. coli* RIL/pET-28a. The results suggested that the introduction of GDH into *E. coli* RIL had almost no effect on cell growth properties, which is similar to the results reported by Yamamoto *et al* [26]. A coupled-system *E. coli* RIL/pET-R-SD-AS-G based on GDH and RCR involved in the reaction of 2-HAP to (*R*)-PED would be preferable for further studies of enzyme-catalyzed biotransformations. As Pennacchio *et al*. reported, the introduction of glucose/gluconic acid into an asymmetric reduction by the cofactor-regeneration enzyme GDH did not interfere with the chiral synthesis [23].

Insert Fig. 2

3.4 The function rebalance of RCR and GDH through their protein-expression optimization

Since the coupled-system *E. coli* RIL/pET-R-SD-AS-G contains two enzymes, RCR and GDH, the protein expression conditions will be optimized to improve their protein expression level and (*R*)-PED biotransformation efficiency. The results showed

E. coli RIL/pET-R-SD-AS-G catalyzed the biosynthesis of (*R*)-PED with a high optical purity of 96.3% and yield of 68.2% when its OD_{600} value reached 1.0 (Fig. 3A). With the increase of IPTG concentration, the optical purity and yield of (*R*)-PED by *E. coli* RIL/pET-R-SD-AS-G were improved and reached the highest level: an optical purity of 96.5% and a yield of 83.2% with 0.4 mM IPTG (Fig. 3B). When IPTG concentration over 0.4 mM was added, the recombinant cells produced (*R*)-PED with a low optical purity and a low yield, which might be due to the cell-growth inhibition resulting in low protein expression. After the addition of 0.4 mM IPTG, the recombinant cells were continue to culture at 37°C for 10 h, the harvested cells catalyzed the biotransformation of (*R*)-PED with the highest efficiency with optical purity of 96.9% in a yield of 94.8% (Fig. 3C, Fig. 3D). Thus, under the optimal expression conditions: OD_{600} 1.0, 0.4 mM IPTG, induce duration 10 h, and the culture temperature 37°C after IPTG induction, the recombinant *E. coli* RIL/pET-R-SD-AS-G catalyzed the biotransformation of (*R*)-PED with an optical purity of 96.9% in a yield of 94.8%.

Insert Fig. 3

3.5 Kinetics demonstrates the good balance between RCR and GDH in coupling system

Since the recombinant RCR was tagged with N-terminal 6×histine, and GDH was fused with C-terminal 6×histine, they were both purified by one-step Ni-affinity chromatography. SDS-PAGE analysis showed that two enzymes: RCR and GDH were

simultaneously purified from the recombinant strain *E. coli* RIL/pET-R-SD-AS-G (Fig. 4), with the corresponding molecular of 30 kDa and 44 kDa. The purified proteins exhibited specific activity of 17.8 Umg^{-1} for 2-HAP reduction, and 21.5 Umg^{-1} for glucose oxidation. The kinetic parameters were determined for 2-HAP or glucose at different concentrations (0.05–0.5 mM) and cofactors at various concentrations (0.05–0.5 mM). As shown in Table 3, the purified RCR and GDH from *E. coli* RIL/pET-R-SD-AS-G showed the similar catalytic efficiency (k_{cat}/K_M) with the purified RCR from *E. coli* RIL/pET-RCR towards 2-HAP, suggesting the co-expression of RCR with GDH had no effects on the function of RCR. The k_{cat}/K_M values of the enzyme RCR and GDH was 3.2 for the reduction of 2-HAP to release NAD^+, and 3.9 for the oxidation of glucose to form NADH. The ratio of k_{cat}/K_M for RCR and GDH catalyzing 2-HAP and glucose was about 1.0, showing the good balance between the functions of RCR and GDH. *C. parapsilosis* RCR and *Bacillus* sp. XY-1 GDH are both homotetramer structures and each molecular of RCR or GDH consists of one NADH or NAD^+.[30, 39]. So, in one reaction, the reduction of NADH and oxidation of NAD^+ by the coupled system containing RCR and GDH almost kept the good rebalance between NAD^+-NADH recycling. These results further confirmed the protein expression optimization is available to rebalance cofactor pathway to improve the biotransformation efficiency of (*R*)-PED by the coupled system. In general, the higher initial reaction rate induced an increase of optical purtity of (*R*)-PED. The introduction of glucose dehydrogenase stimulated the improved reaction rate, resulting in an increase of optical purtity of (*R*)-PED [20, 22].

Insert Table 3

Insert Fig.4

3.6 Improving (*R*)-PED biotransformation through pH and temperature optimization

In enzyme-mediated reaction, with the increase of temperature, the activity of protein is reduced, resulting in the decrease of reaction rate [37]. On the other hand, temperature sometimes changes the product stereoselectivity during enzyme-catalyzed chiral biosynthesis [40]. As showed in Fig.5A, with the increase of temperature lower than 35°C, the bioconversion efficiency of (*R*)-PED from 2-HAP by the coupled system was increased and reached the highest level: an optical purity of 98.2% and a yield of 97.4% at 35°C.

The pH value affects the dissociation degree of the groups in the enzyme active center, substrate and coenzyme, thus changes the binding strength between enzyme and substrate [41]. When the pH is 7.5, the recombinant strain *E. coli* RIL/pET-R-SD-AS-G catalyzes the biotransformation of (*R*)-PED with the highest optical purity of 99.0% and yield of 98.5% (Fig.5B).

During the biotransformation process by the coupled system *E. coli* RIL/pET-R-SD-AS-G, the reaction duration was also investigated targeting the highest optical purity and yield of (*R*)-PED under optimal temperature and pH. The results showed that the optical purity and yield of (*R*)-PED both reached 99.9% in 24 h (Fig.5C). Compared to *E. coli*/RCR, the reaction duration was significantly reduced

two fold: from 48 h to 24 h [34,38]. So the coupled system based on RCR and GDH efficiently catalyzes (*R*)-PED biosynthesis with almost absolute stereochemical selectivity. The reduced yield of (*R*)-PED at 30 h may be due to the slightly higher catalytic efficiency of GDH (k_{cat}/K_M is 3.9) than that of RCR (k_{cat}/K_M is 3.2), resulting more NAD^+ for RCR catalyzing (*R*)-PED to 2-HAP. As reported by Xiao *et al.*, the introduction of cofactor-recycling enzyme into the asymmetric reaction system significantly improves the chiral biosynthesis efficiency [24]. Pennacchio *et al.* recently evaluated asymmetric reduction of α-keto esters with *Thermus thermophilus* NADH-dependent carbonyl reductase using GDH for cofactor-regeneration enzyme [22]. The strengthened cofactor regeneration can overcome coenzyme restriction in the asymmetric reduction and accelerate the initial reaction rate, resulting in improved chiral biosynthesis efficiency [23-25, 27].

Insert Fig. 5

4. Conclusions

The NADH-dependent *E. coli*-RCR catalyzes the reduction 2-HAP to (*R*)-PED with low efficiency. To improve the biotransformation efficiency of (*R*)-PED, the cofactor-regeneration enzyme GDH was introduced into (*R*)-PED biosynthesis pathway in three different *E. coli* hosts. Among three coupled systems, *E. coli* RIL/pET-R-SD-AS-G showed the higher specific activity with 2-HAP and biotransformation efficiency of (*R*)-PED than *E. coli* BL21/pET-R-SD-AS-G and *E. coli* Rosetta/pET-R-SD-AS-G. The two enzymes' functions were rebalanced through

protein-expression optimization. The kinetic demonstrated the good balance between the functions of RCR and GDH. At optimum 35°C and pH 7.5, the rebalanced system gave excellent performance in preparation of (*R*)-PED with an optical purity of 99.9% and a yield of 99.9% at 24 h. The introduction of glucose dehydrogenase in *E. coli* RIL/pET-R-SD-AS-G stimulated increases of 23.8% and 63.8%, respectively, in optical purity and yield, and simultaneously reduced the reaction time two-fold (from 48 h to 24 h). This work provides a valuable enzyme-coupled method for efficient chiral biosynthesis through protein-expression and biotransformation optimization to rebalance cofactor pathways.

Acknowledgements

This project was supported by the National Science Foundation of China (31370100), Jiangsu Province Basic Research Program (BK20131101), the Program for New Century Excellent Talents in Universities (NCET-13-0833), the Fundamental Research Funds for the Central Universities (JUSRP51409B),, the National Key Basic Research and Development 973 Program of China (2011CB710800), and the Program of Introducing Talents of Discipline to Universities (111-2-06), a Project Funded by the Priority Academic Program Development of Jiangsu Higher Education Institutions.

References

[1] Schmid A, Dordick JS, Hauer B, Kiener A, Wubbolts M, Witholt B. Industrial biocatalysis today and tomorrow. Nature 2001;409:258-268.

[2] Pollard DJ, Woodley JM. Biocatalysis for pharmaceutical intermediates: the future is now. Trends in Biotechnology 2007;25:66-73.

[3] Pandey RK, Fernandes RA, Kumar P. An asymmetric dihydroxylation route to enantiomerically pure norfluoxetine and fluoxetine. Tetrahedron Letters 2002;43:4425-4426.

[4] Hammond RJ, Poston BW, Ghiviriga I, Feske BD. Biocatalytic synthesis towards both antipodes of 3-hydroxy-3-phenylpropanitrile a precursor to fluoxetine, atomoxetine and nisoxetine. Tetrahedron Letters 2007;48:1217-1219.

[5] Kalaitzakis D, Rozzell JD, Smonou I, Kambourakis S. Synthesis of valuable chiral intermediates by isolated ketoreductases: Application in the synthesis of alpha-alkyl-beta-hydroxy ketones and 1,3-diols. Advanced Synthesis & Catalysis 2006;348:1958-1969.

[6] Katzberg M, Wechler K, Mueller M, Duenkelmann P, Stohrer J, Hummel W, Bertau M. Biocatalytical production of (5*S*)-hydroxy-2-hexanone. Organic & Biomolecular Chemistry 2009;7:304-314.

[7] Huang Y, Liu N, Wu X, Chen Y. Dehydrogenases/Reductases for the synthesis of chiral pharmaceutical intermediates. Current Organic Chemistry 2010;14:1447-1460.

[8] Patel RN. Biocatalytic synthesis of intermediates for the synthesis of chiral drug substances. Current Opinion in Biotechnology 2001;12:587-604.

[9] Patel RN. Biocatalysis: Synthesis of key intermediates for development of pharmaceuticals. Acs Catalysis 2011;1:1056-1074.

[10] Yasohara Y, Kizaki N, Hasegawa J, Wada M, Kataoka M, Shimizu S. Molecular cloning and overexpression of the gene encoding an NADPH-dependent carbonyl reductase from *Candida magnoliae*, involved in stereoselective reduction of ethyl 4-chloro-3-oxobutanoate. Bioscience Biotechnology and Biochemistry 2000;64:1430-1436.

[11] Wang SS, Xu Y, Zhang RZ, Zhang BT, Xiao R. Improvement of (*R*)-carbonyl reductase-mediated biosynthesis of (*R*)-1-phenyl-1,2-ethanediol by a novel dual-cosubstrate-coupled system for NADH recycling. Process Biochemistry 2012;47:1060-1065.

[12] Zhang RZ, Xu Y, Geng YW, Wang SS, Sun Y, Xiao R. Improved production of (*R*)-1-phenyl-1,2-ethanediol by a codon-optimized (*R*)-specific carbonyl reductase from *Candida parapsilosis* in *Escherichia coli.* Applied Biochemistry and Biotechnology 2010;160:868-878.

[13] Salvi NA, Chattopadhyay S. Studies on *Rhizopus arrhizus* mediated enantioselective reduction of arylalkanones. Tetrahedron 2001;57:2833-2839.

[14] Zilbeyaz K, Kurbanoglu EB. Highly rnantiomeric reduction of acetophenone and its derivatives by locally isolated *Rhodotorula glutinis.* Chirality 2010;22:849-854.

[15] Kurbanoglu EB, Zilbeyaz K, Kurbanoglu NI, Kilic H. Enantioselective reduction of substituted acetophenones by *Aspergillus niger.* Tetrahedron-Asymmetry 2007;18:1159-1162.

[16] Mandal D, Ahmad A, Khan MI, Kumar R. Enantioselective bioreduction of acetophenone and its analogous by the fungus *Trichothecium* sp. Journal of Molecular Catalysis B-Enzymatic 2004;27:61-63.

[17] Soni P, Banerjee UC. Enantioselective reduction of acetophenone and its derivatives with a new yeast isolate *Candida tropicalis* PBR-2 MTCC 5158. Biochemical Journal 2006;1:80-85.

[18] Lavandera I, Kern A, Ferreira-Silva B, Glieder A, de Wildeman S, Kroutil W. Stereoselective bioreduction of bulky-bulky ketones by a novel ADH from *Ralstonia sp.* Journal of Organic Chemistry 2008;73:6003-6005.

[19] Zhao, H. and W. A. van der Donk. Regeneration of cofactors for use in biocatalysis. Current Opinion in Biotechnology 2003;14(6):583-589.

[20] Yamamoto H, Mitsuhashi K, Kimoto N, Kobayashi Y, Esaki N. Robust NADH-regenerator: improved

412 alpha-haloketone-resistant formate dehydrogenase. Applied Microbiology and Biotechnology
413 2005;67:33-39.
414 [21] Gröger H, Hummel W, Rollmann C, Chamouleau F, Husken H, Werner H, Wunderlich C, Abokitse K,
415 Drauz K, Buchholz S. Preparative asymmetric reduction of ketones in a biphasic medium with an
416 (*S*)-alcohol dehydrogenase under in situ-cofactor-recycling with a formate dehydrogenase.
417 Tetrahedron 2004;60:633-640.
418 [22] Wada M, Yoshizumi A, Noda Y, Kataoka M, Shimizu S, Takagi H, Nakamori S. Production of a
419 doubly chiral compound, (4*R*,6*R*)-4-hydroxy-2,2,6-trimethylcyclohexanone, by two-step enzymatic
420 asymmetric reduction. Applied and Environmental Microbiology 2003;69:933-937.
421 [23] Pennacchio A, Giordano A, Rossi M, Raia CA. Asymmetric reduction of alpha-keto esters with
422 *Thermus thermophilus* NADH-dependent carbonyl reductase using glucose dehydrogenase and
423 alcohol dehydrogenase for cofactor regeneration. European Journal of Organic Chemistry
424 2011:4361-4366.
425 [24] Zhang RZ, Zhang BT, Xu Y, Li YH, Li M, Liang HB, Xiao R. Efficicent (*R*)-phenylethanol production
426 with enantioselectivity-alerted (*S*)-carbonyl reductase II and NADPH regeneration. PLoS One
427 2013;8:e83586.
428 [25] Xu Z, Jing K, Liu Y, Cen P. High-level expression of recombinant glucose dehydrogenase and its
429 application in NADPH regeneration. Journal of Industrial Microbiology & Biotechnology
430 2007;34:83-90.
431 [26] Yamamoto H, Mitsuhashi K, Kimoto N, Matsuyama A, Esaki N, Kobayashi Y. A novel
432 NADH-dependent carbonyl reductase from kluyveromyces aestuarii and comparison of
433 NADH-regeneration system for the synthesis of ethyl (*S*)-4-chloro-3-hydroxybutanoate. Bioscience
434 Biotechnology and Biochemistry 2004;68:638-649.
435 [27] Geng YW, Zhang RZ, Xu Y, Wang SS, Sha C, Xiao R. Coexpression of a carbonyl reductase and
436 glucose 6-phosphate dehydrogenase in *Pichia pastoris* improves the production of
437 (*S*)-1-phenyl-1,2-ethanediol. Biocatalysis and Biotransformation 2011;29:172-178.
438 [28] Xiao Z, Lv C, Gao C, Qin J, Ma C, Liu Z, Liu P, Li L, Xu P. A novel whole-cell biocatalyst with NAD(+)
439 regeneration for production of chiral chemicals. Plos One 2010;5:e8860.
440 [29] Ye Q, Cao H, Zang GL, Mi L, Yan M, Wang Y, Zhang YY, Li XM, Li JA, Xu L, Xiong JA, Ouyang PK, Ying
441 HJ. Biocatalytic synthesis of (*S*)-4-chloro-3-hydroxybutanoate ethyl ester using a recombinant
442 whole-cell catalyst. Applied Microbiology and Biotechnology 2010;88:1277-1285.
443 [30] Kosjek B, Nti-Gyabaah J, Telari K, Dunne L, Moore JC. Preparative asymmetric synthesis of
444 4,4-dimethoxytetrahydro-2H-pyran-3-ol with a ketone reductase and in situ cofactor recycling
445 using glucose dehydrogenase. Organic Process Research & Development 2008;12:584-588.
446 [31] Kizaki N, Yasohara Y, Hasegawa J, Wada M, Kataoka M, Shimizu S. Synthesis of optically pure ethyl
447 (*S*)-4-chloro-3-hydroxybutanoate by *Escherichia coli* transformant cells coexpressing the carbonyl
448 reductase and glucose dehydrogenase genes. Applied Microbiology and Biotechnology
449 2001;55:590-595.
450 [32] Nie Y, Xu Y, Lv TF, Xiao R. Enhancement of *Candida* parapsilosiscatalyzing deracemization of
451 (*R*,*S*)-1-phenyl-1, 2-ethanediol: agitation speed control during cell cultivation. Journal of Chemical
452 Technology & Biotechnology 2009;84:468-472.
453 [33] Zhang RZ, Xu Y, Xiao R, Wang SS, Zhang BT. Improved production of (*R*)-1-phenyl-1,2-ethanediol
454 using *Candida parapsilosis* (*R*)-carbonyl reductase expressed in *Pichia pastoris.* Process
455 Biochemistry 2011;46:709-713.

[34] Wang SS, Nie Y, Xu Y, Zhang RZ, Ko TP, Huang CH, Chan HC, Guo RT, Xiao R. Unconserved substrate-binding sites direct the stereoselectivity of medium-chain alcohol dehydrogenase. Chemical Communications 2014;50:7770-7772.

[35] Nie Y, Xu Y, Wang HY, Xu Na, Xiao R. Synthesis of (*R*)-1-phenyl-1,2-ethanediol by stereospecific reduction of 2-hydroxyacetophenone using recombinant *Escherichia coli* expressing (*R*)-specific carbonyl reductase. Chemical Industry and Engineering Progress. 2006;25:1231-1236.

[36] Zhao HM, van der Donk WA. Regeneration of cofactors for use in biocatallysis. Current Opinion in Biotechnology 2003;14:583-589.

[37] Zhang RZ, Xu Y, Wang SS, Zhang BT, Geng Y. Expression and subcellular localization of (*R*)- and (*S*)-specific carbonyl reductases from *Candida parapsilosis* in *Saccharomyces cerevisia.* Acta Microbiologica Sinica 2011;51:789-795.

[38] Ho SN, Hunt HD, Horton RM, Pullen JK, Pease LR. Site-directed mutagenesis by overlap extension using the polymerase chain reaction. Gene 1989;77:51-9.

[39] Nie Y, Xu Y, Mu XQ, Wang HY, Yang M, Xiao R. Purification, characterization, gene cloning, and expression of a novel alcohol dehydrogenase with anti-prelog stereospecificity from *Candida parapsilosis.* Applied and Environmental Microbiology 2007;73:3759-3764.

[40] Zhang RZ, Xu Y, Sun Y, Zhang WC, Xiao R. Ser67Asp and His68Asp substitutions in *candida parapsilosis* carbonyl reductase alter the coenzyme specificity and enantioselectivity of ketone reduction. Applied and Environmental Microbiology 2009;75:2176-2183.

[41] Yamamoto K, Kurisu G, Kusunoki M, Tabata S, Urabe I, Osaki S. Crystal structure of glucose dehydrogenase from *Bacillus megaterium* IWG3 at 1.7 angstrom resolution. Journal of Biochemistry 2001;129:303-312.

[42] Ni Y, Li CX, Wang LJ, Zhang J, Xu JH. Highly stereoselective reduction of prochiral ketones by a bacterial reductase coupled with cofactor regeneration. Organic & Biomolecular Chemistry 2011;9:5463-5468.

[43] Klimacek M, Nidetzky B. The oxyanion hole of *Pseudomonas fluorescens* mannitol 2-dehydrogenase: a novel structural motif for electrostatic stabilization in alcohol dehydrogenase active sites. Biochemical Journal 2010;425:455-463.

Figure captions:

Fig. 1 SDS-PAGE analysis of protein expression in the recombinant strains. 1. *E. coli* RIL/pET-R-SD-AS-G induced with 0.1 mM IPTG; 2. *E. coli* RIL/pET-R-SD-AS-G without IPTG; 3. *E. coli* Rosetta/pET-R-SD-AS-G induced with 0.1 mM IPTG; 4. *E. coli* BL21/pET- R-SD-AS-G induced with 0.1 mM IPTG; 5. *E. coli* BL21/pET-28a induced with 0.1 mM IPTG; M. Protein marker.

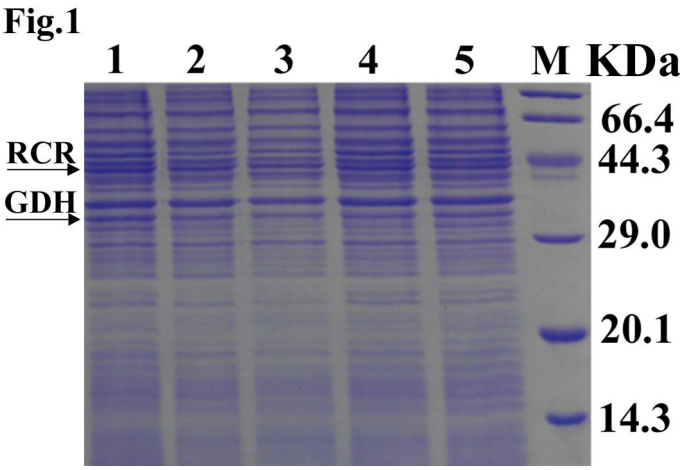

Fig. 2 Cell-growth curve of the recombinant strains.

The recombinant strains were cultivated at 37°C in 2.5-L flask bottles, with an initial working volume of 1.0 L, and then 0.1 mM IPTG was added at 4 h to induce protein expression. Error bars represent standard deviations (n = 3).

Fig.2

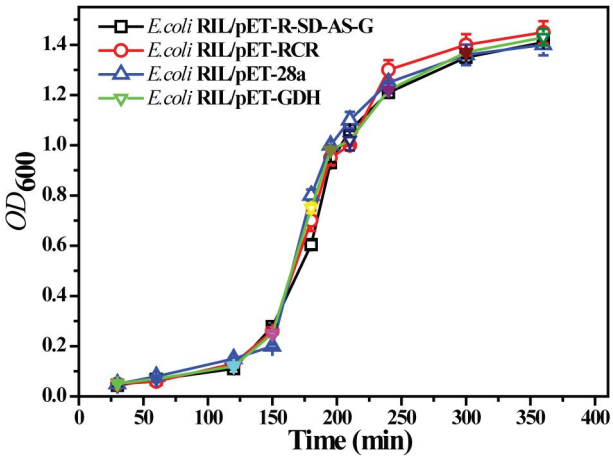

496

497 **Fig. 3 The effects of expression conditions on transformation efficiency of**

498 **(*R*)-PED**

499 The recombinant *E. coli* RIL/pET-R-SD-AS-G were cultured under the different

500 protein expression conditions of RCR and GDH: OD_{600} value (0.4–1.5) of the culture,

501 IPTG concentrations (0.2–2.0 mM), induce temperature (17°C–37°C), induce times

502 (8–20 h). The recombinant cells were collected for the biotransformation of (*R*)-PED

503 in 0.1 M potassium phosphate buffer (pH 7.0) at 35°C.

504

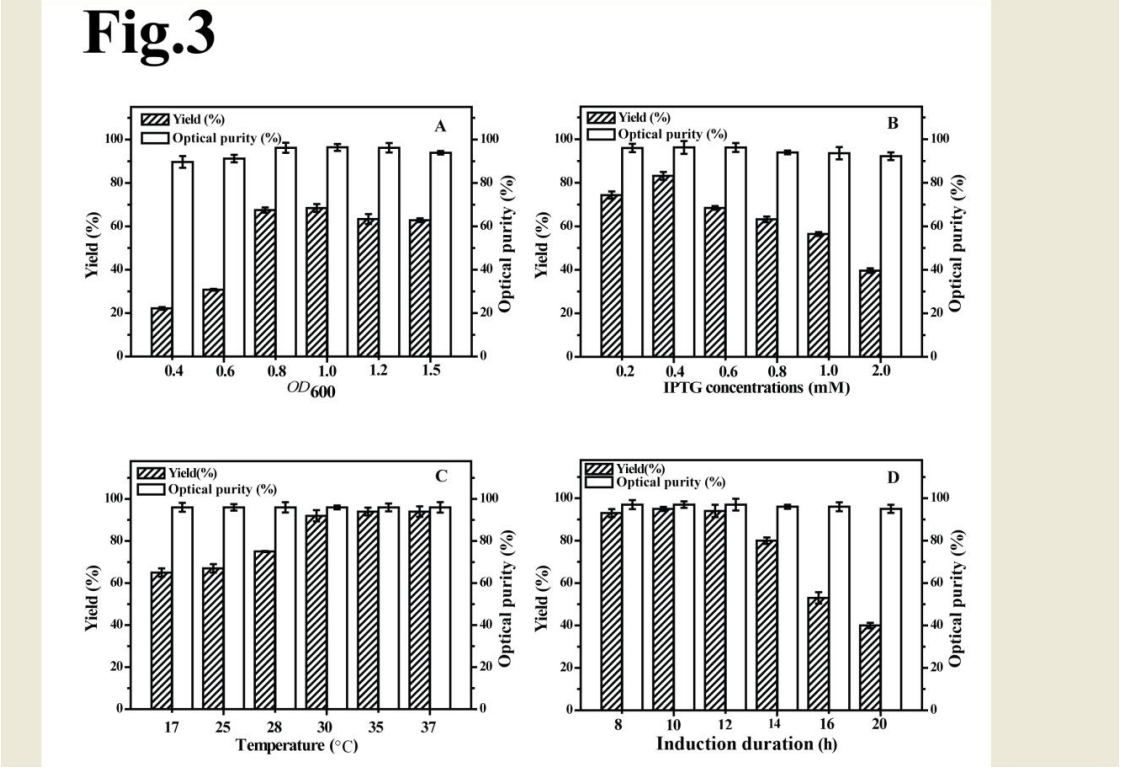

Fig. 4 SDS-PAGE analysis of purified RCR and GDH from the coupled system. 1. Elution with 300 mM imidazole; 2. Cell-free extracts of *E. coli* RIL/pET-R-SD-AS-G; 3. Whole-cells of *E. coli* RIL/pET-R-SD-AS-G with 0.5 mM IPTG; M. Protein marker.

Fig.4

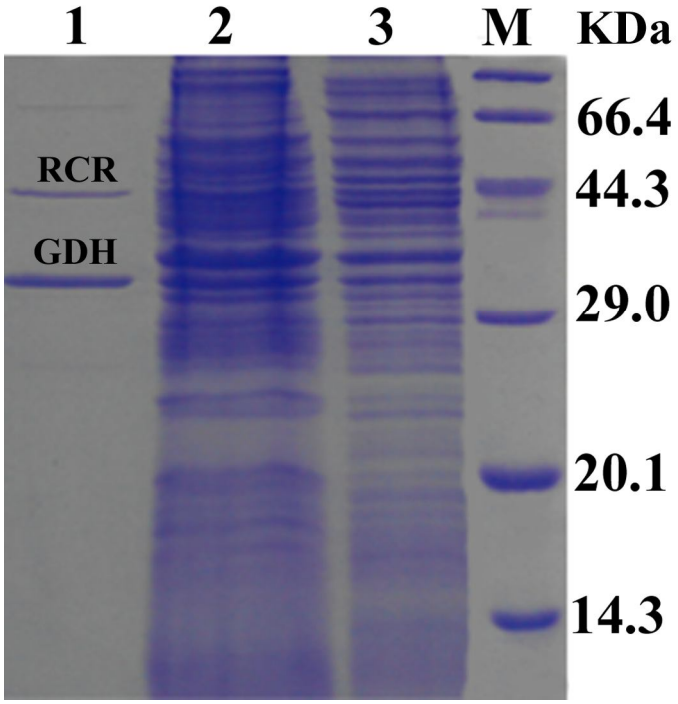

Fig.5 Optimal pH and temperature for whole-biocatalyst biotransformation.

The pH optimum of (*R*)-PED transformation was determined between pH 4.0 and 10.0 using 0.1 M citric acid buffer (pH 4.0, 4.5, 5.0, 5.5), 0.1 M potassium phosphate buffer (pH 6.0, 6.5, 7.0, 7.5), 50 mM Tris-HCl buffer (8.0), and 0.1 M carbonate buffer (pH 9.0, 10.0). The temperature optimum of (*R*)-PED transformation was determined at various temperatures (20°C–80°C).

Fig.5

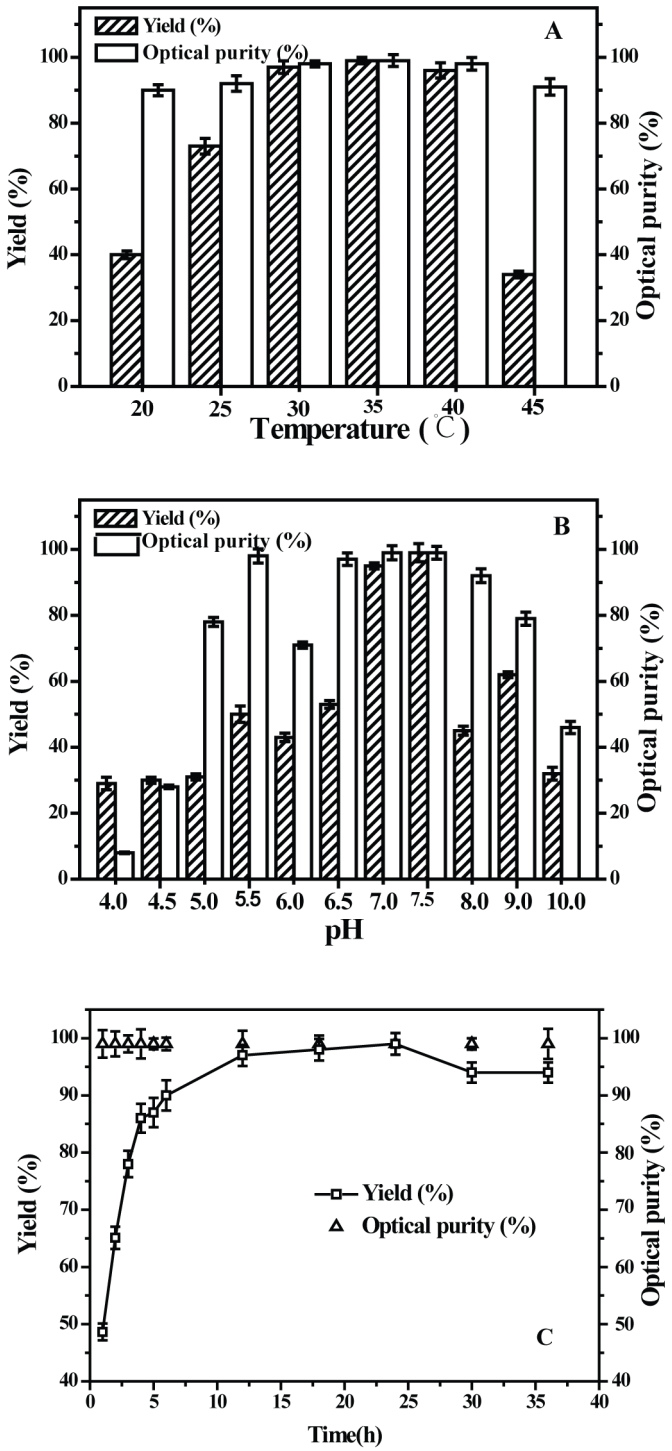

517

518 **Table1**

519 Strains, plasmids and primers

Strains, plasmids and primers	Characteristics	Source
Strains		
E. coli JM 109/ T-R-SD-AS-G	*E. coli* JM 109 harboring pET-R-SD-AS-G	This work
E. coli BL21/ pET-R-SD-AS-G	*E. coli* BL21 harboring pET-R-SD-AS-G	This work
E. coli RIL/pET-R-SD-AS-G	*E. coli* RIL harboring pET-R-SD-AS-G	This work
E. coli Rosseta/ pET-R-SD-AS-G	*E. coli* Rosseta harboring pET-R-SD-AS-G	This work
Plasmids		
pET-RCR	The donor of RCR gene	This lab
pET-GDH	The donor of GDH gene	This lab
pMD19-T	Cloning plasmid, 2.7 kb, Amp^r	Takara Co.
T-R-SD-AS-G	R-SD-AS-G genes on pMD19-T, 4.5 kb	This work
pET-R-SD-AS-G	R-SD-AS-G gene on pET-28, 7.5 kb	This work
Primers	Sequence (5'→3')	
R-SD-AS-G-f	ATCCTGCTAGCATGTCAATTCCATCAAGCCAGTAC（*Nhe*I）	
R-SD-AS-G-r	TGACTCTCGAGACCGCGGCCTGCCTG（*Xho*I）	
RCR-r	CGGATACAT**GGTATATCTCCTTC**CTATGGATTAAAAACAACTCTACCTT	
GDH-f	AATCCATAG**GAAGGAGATATACC**ATGTATCCGGATTTAAAAGGAAAA GTC	

520 **Notes:** The sequence of SD-AS is bold; the restriction endonuclease sites are underlined.

521

522 **Table 2**

523 Enzyme activities in cell-free extracts of recombinant strains

Recombinant strains	Specific activities (Umg^{-1})		Biotransformation	
	Reductive activities with 2-HAP (Umg^{-1})	Oxidative activities with glucose (Umg^{-1})	Optical purity (%)	Yield (%)
E. coli BL21/pET-R-SD-AS-G	0.6±0.02	1.1±0.01	87.9±0.9	60.2±0.2
E. coli RIL/pET-R-SD-AS-G	0.6±0.01	1.3±0.02	96.1±1.2	63.8±0.7
E.coli Rosetta/pET-R-SD-AS-G	0.4±0.01	0.9±0.01	45.1±1.2	20.4±0.3

524 **Notes:** The biotransformations were carried out at 0.1 M potassium phosphate buffer (pH 7.0),

525 35°C with 6 gL^{-1} 2-HAP as substrate.

526

Table 3

Kinetic parameters for 2-HAP and glucose by the purified RCR and GDH in *E. coli* RIL[a]

Enzymes[b]	Specific activity (Umg^{-1})	K_M (μM)	k_{cat} (s^{-1})	k_{cat}/K_M ($\times 10^6 s^{-1}M^{-1}$)
E. coli RIL/$RCR_{2\text{-}HAP}$	18.5	5.3±0.2	18.1±0.3	3.4
E. coli RIL/$RCR_{glucose}$	ND	ND[c]	ND	ND
E. coli RIL/RCR-$GDH_{2\text{-}HAP}$	17.8	4.5±0.1	14.2±0.2	3.2
E. coli RIL/RCR-$GDH_{glucose}$	21.5	31.4±0.3	122.5±0.7	3.9

Notes: The recombinant RCR was purified from *E. coli* RIL/RCR, and the coupled enzyme RCR-GDH was purified from *E. coli* RIL/pET-R-SD-AS-G using His Trap HP affinity chromatography.

[a] All reactions involved in the calculation of kinetic constants calculation were assayed at 0.1 M potassium phosphate buffer (pH 7.0) and 35°C. All experiments were repeated three times.

[b] $RCR_{2\text{-}HAP}$ ($RCR_{glucose}$) means the purified RCR with 2-HAP (glucose) as substrate; RCR-$GDH_{2\text{-}HAP}$ ($RCR_{glucose}$) means the purified coupled RCR-GDH with 2-HAP (glucose) as substrate.

[c] ND, not detected.